

# Kinetics of Self-Immolation: Faster Signal Relay over a Longer Linear Distance?

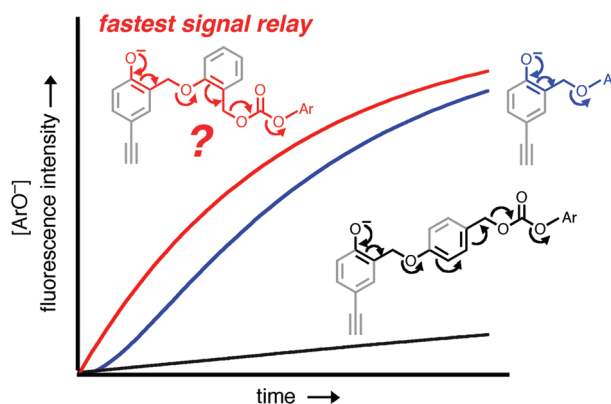
Ho Yong Lee, Xuan Jiang, and Dongwhan Lee\*

Department of Chemistry, Indiana University, 800 East Kirkwood Avenue,  
Bloomington, Indiana 47405

dongwhan@indiana.edu

Received March 2, 2009

## ABSTRACT

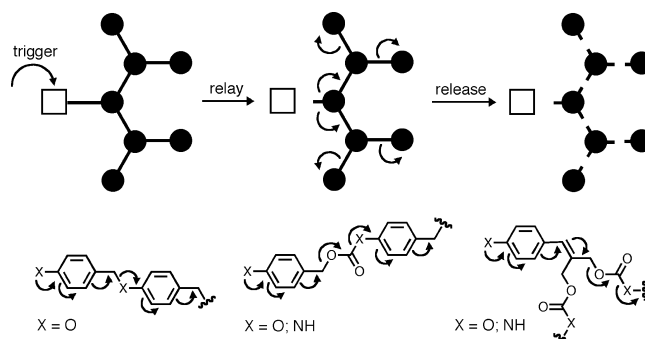


A counterintuitive observation of a *faster signal relay* over a *longer linear distance* prompted detailed kinetic studies of self-immolation reactions. With appropriate conformational bias, trigger-to-reporter signal transduction can take an efficient “shortcut” that outperforms conventional pathways involving repetitive quinone methide rearrangements and elimination.

Chemical structures that can amplify and transmit externally triggered structural changes over a long distance are critical functional components in signal transduction.<sup>1</sup> Controlled chain fragmentation of self-immolative molecules is one drastic chemical mode of operation that satisfies such criteria. Here, repetitive bond rearrangement reactions following a single triggering event propagate through the molecular backbone to release remotely located signaling units (Scheme 1).<sup>2–5</sup> The self-immolative nature of one such motif, quinone methide (QM), has been extensively exploited within this context.

Since the seminal independent studies that appeared in the literature in 2003,<sup>3a,4a,b,5</sup> numerous prototypes of signal-amplifying self-immolative sensors and drug delivery ve-

**Scheme 1.** Mechanism of Self-Immolation and Representative Structural Motifs Undergoing Sequential Bond Cleavage Reactions

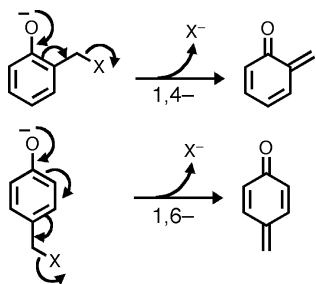


(1) Kay, E. R.; Leigh, D. A.; Zerbetto, F. *Angew. Chem., Int. Ed.* **2007**, 46, 72–191.

(2) (a) Wang, W.; Alexander, C. *Angew. Chem., Int. Ed.* **2008**, 47, 7804–7806. (b) Shabat, D. *J. Polym. Sci., Part A: Polym. Chem.* **2006**, 44, 1569–1578.

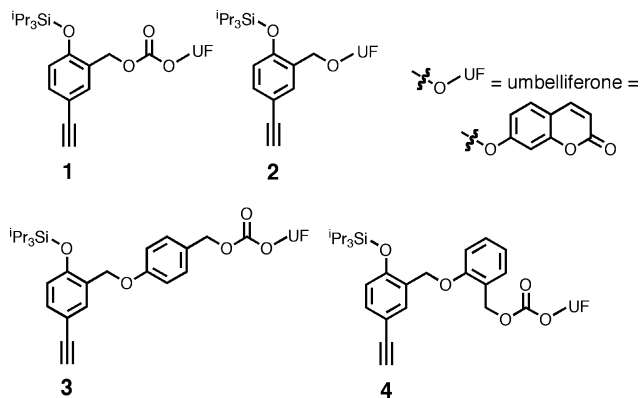
hicles have been reported.<sup>3–5</sup> However, surprisingly little is known about the structure–reactivity relationships underpinning the mechanism of signal relay, including the rearrangement kinetics of QM itself (Scheme 2).<sup>6</sup> In this paper, we

**Scheme 2.** Self-Fragmentation through 1,4- (top) and 1,6-Rearrangement (bottom)



describe mechanistic studies on well-defined trigger–relay–reporter conjugates that undergo externally triggered chain fragmentation. Our kinetic evidence points toward an alternative mechanism of self-immolation, by which a signal travels to distant positions through a reaction pathway that does not necessarily involve repetitive bond rearrangements. In addition to dictating the kinetics of trigger-to-reporter signal transduction, the chemical structure of the linker units profoundly influenced the mechanism of chain fragmentation, which has significant implications for the rational design of stimuli-responsive molecules and materials.

Our mechanistic investigation of QM rearrangement was prompted by the kinetic behavior of the compounds **1** and **2**. These molecules were designed specifically to integrate (i) a Si–O group to be cleaved by F<sup>−</sup> anion functioning as the triggering agent,<sup>7</sup> (ii) a carbonate- (for **1**) or ether-extended (for **2**) 1,2-QM linker as a signal relay, (iii) a “masked” umbelliferone (7-hydroxycoumarin) unit to be released as the final product and to elicit turn-on fluorescence response,<sup>8</sup> and (iv) an ethynyl group as an anchoring point for future immobilization studies.



In THF at 293 K, **1** showed broad UV–vis absorptions at  $\lambda < 360$  nm but remained essentially nonemissive. Upon reaction with F<sup>−</sup> (100 equiv, delivered as TBAF salt),

however, the solution turned yellow with the appearance of strong ( $\epsilon = 23\,000\text{ M}^{-1}\text{ cm}^{-1}$ ) absorption at  $\lambda_{\text{max,abs}} = 407$  nm and development of blue emission at  $\lambda_{\text{max,em}} = 455$  nm, indicating quantitative release of umbelliferone as the final product of the reaction (Figure 1a and Scheme 3). Under similar conditions, **2** reacted similarly with F<sup>−</sup>, but its

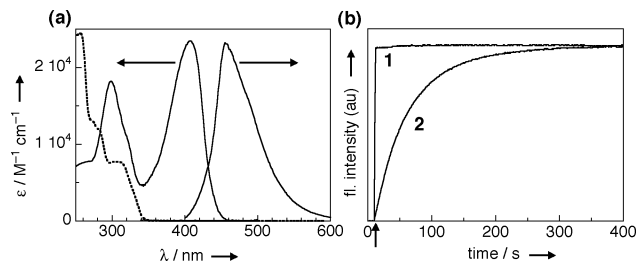


**Figure 1.** (a) UV–vis and emission spectra of **1** prior to (dotted lines;  $\lambda_{\text{exc}} = 300$  nm) and after (solid lines;  $\lambda_{\text{exc}} = 380$  nm) reaction with F<sup>−</sup> (100 equiv) in THF. (b) Time-dependent changes in the fluorescence intensity of **1** and **2** monitored at  $\lambda = 460$  nm ( $\lambda_{\text{exc}} = 380$  nm) after addition of F<sup>−</sup> (100 equiv) at  $t = 10$  s (indicated by a gray arrow).  $T = 293$  K.

response kinetics was strikingly different from that of **1** (Figure 1b). Apparently, the release of CO<sub>2</sub> as part of the chain fragmentation cascade provides additional thermodynamic driving force that is responsible for the experimentally observed faster kinetic response of **1** relative to **2**.

To derive kinetic parameters associated with each step in the chain fragmentation (Scheme 3), subsequent measurements were conducted in CH<sub>2</sub>Cl<sub>2</sub>. Under pseudo-first-order conditions, an exponential increase in the emission intensity was observed from **1** + F<sup>−</sup> at 293 K (Figures 2a and S1, Supporting Information).<sup>9</sup> A linear dependence of the pseudo-first-order rate constant  $k_1'$  ( $= k_1[\text{F}^-]_0$ ; eq 1) on  $[\text{F}^-]_0$  (Figure S2, Supporting Information)

(3) (a) Amir, R. J.; Pessah, N.; Shamis, M.; Shabat, D. *Angew. Chem., Int. Ed.* **2003**, *42*, 4494–4499. (b) Shamis, M.; Lode, H. N.; Shabat, D. *J. Am. Chem. Soc.* **2004**, *126*, 1726–1731. (c) Amir, R. J.; Shabat, D. *Chem. Commun.* **2004**, 1614–1615. (d) Amir, R. J.; Popkov, M.; Lerner, R. A.; Barbas, C. F., III; Shabat, D. *Angew. Chem., Int. Ed.* **2005**, *44*, 4378–4381. (e) Amir, R. J.; Danieli, E.; Shabat, D. *Chem.–Eur. J.* **2007**, *13*, 812–821. (f) Shamis, M.; Shabat, D. *Chem.–Eur. J.* **2007**, *13*, 4523–4528. (g) Sagi, A.; Weinstein, R.; Karton, N.; Shabat, D. *J. Am. Chem. Soc.* **2008**, *130*, 5434–5435. (h) Weinstein, R.; Sagi, A.; Karton, N.; Shabat, D. *Chem.–Eur. J.* **2008**, *14*, 6857–6861.

(4) (a) Li, S.; Szalai, M. L.; Kevitch, R. M.; McGrath, D. V. *J. Am. Chem. Soc.* **2003**, *125*, 10516–10517. (b) Szalai, M. L.; Kevitch, R. M.; McGrath, D. V. *J. Am. Chem. Soc.* **2003**, *125*, 15688–15689. (c) McGrath, D. V. *Mol. Pharmaceutics* **2005**, *2*, 253–263.

(5) de Groot, F. M. H.; Albrecht, C.; Koekkoek, R.; Beusker, P. H.; Scheeren, H. W. *Angew. Chem., Int. Ed.* **2003**, *42*, 4490–4494.

(6) (a) de Groot, F. M. H.; Loos, W. J.; Koekkoek, R.; van Berkom, L. W. A.; Busscher, G. F.; Seelen, A. E.; Albrecht, C.; de Bruijn, P.; Scheeren, H. W. *J. Org. Chem.* **2001**, *66*, 8815–8830. (b) Warnecke, A.; Kratz, F. *J. Org. Chem.* **2008**, *73*, 1546–1552. (c) Erez, R.; Shabat, D. *Org. Biomol. Chem.* **2008**, *6*, 2669–2672.

(7) (a) Zhou, Q.; Rokita, S. E. *Proc. Natl. Acad. Sci. U.S.A.* **2003**, *100*, 15452–15457. (b) Weinert, E. E.; Dondi, R.; Colloredo-Melz, S.; Frankenfeld, K. N.; Mitchell, C. H.; Freccero, M.; Rokita, S. E. *J. Am. Chem. Soc.* **2006**, *128*, 11940–11947. (c) Kim, S. Y.; Hong, J.-I. *Org. Lett.* **2007**, *9*, 3109–3112.

(8) (a) Gao, W.; Xing, B.; Tsien, R. Y.; Rao, J. *J. Am. Chem. Soc.* **2003**, *125*, 11146–11147. (b) Meyer, Y.; Richard, J.-A.; Massonneau, M.; Renard, P.-Y.; Romieu, A. *Org. Lett.* **2008**, *10*, 1517–1520.

(9) See Supporting Information.

**Scheme 3.** Stepwise Fragmentation of **1–4** Triggered by Fluoride-Induced Desilylation

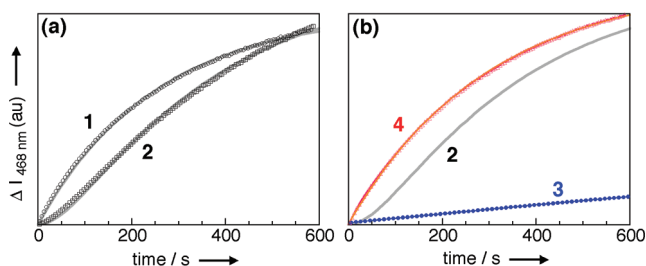
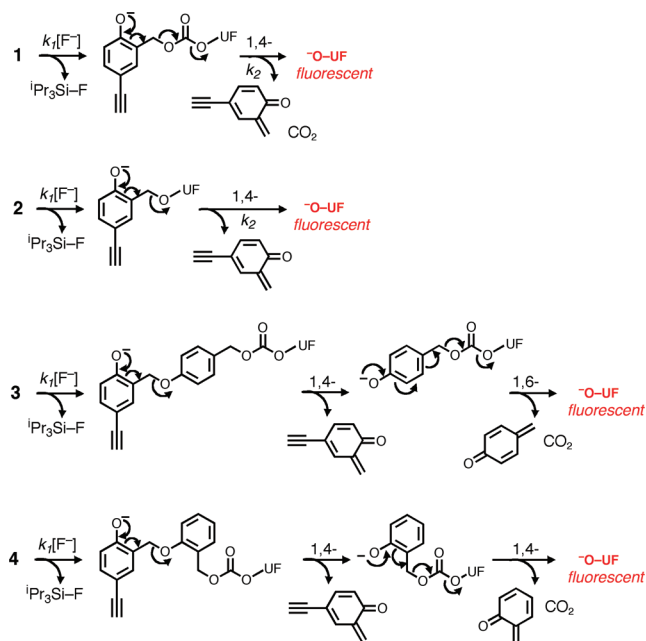


**Figure 2.** Time-dependent changes in the fluorescence intensity at  $\lambda = 460$  nm ( $\lambda_{\text{exc}} = 380$  nm) observed from **1** (open circle), **2** (open square), **3** (filled circle, blue) and **4** (open triangle, red) upon reaction with  $\text{F}^-$  (20 equiv) in  $\text{CH}_2\text{Cl}_2$  at  $T = 293$  K. The gray curves overlaid on the experimental data in (a) are theoretical fits generated using  $k_1 = 155 \text{ M}^{-1} \text{ s}^{-1}$  (for **1** and **2**) and  $k_2 = 1.43 \times 10^{-2} \text{ s}^{-1}$  (for **2**). The fitted curve of **2** is reproduced in (b) for comparison with **3** and **4**.

indicated a rate-determining Si–O bond cleavage by  $\text{F}^-$  with the second-order rate constant of  $k_1 = 155 \text{ M}^{-1} \text{ s}^{-1}$ . This initial bimolecular step is followed by a rapid 1,4-rearrangement (Scheme 3) and subsequent release of  $\text{CO}_2$  and the fluorescent reporter. Here, the requisite phenoxide intermediate apparently builds up only to a very low and steady-state concentration, thus validating the approximation of  $k_1' \ll k_2$  in eq 2 and the use of eq 1 for kinetic modeling (Figure S3, Supporting Information).<sup>10</sup>

(10) Connors, K. A. *Chemical Kinetics: The Study of Reaction Rates in Solution*; Wiley-VCH: Weinheim, 1990.

$$\frac{\Delta I}{I} = 1 - e^{-k_1' t} \quad (1)$$

$$\frac{\Delta I}{I} = \frac{1}{k_2 - k_1'} \{k_2 (1 - e^{-k_1' t}) - k_1' (1 - e^{-k_2 t})\} \quad (2)$$

Under similar conditions, however, the fluorescence enhancement from **2** showed a markedly different kinetic behavior (Figure 2a). Specifically, the early induction period<sup>3c–f</sup> consistently observed under pseudo-first-order reaction conditions (Figures 2a and S3–S4, Supporting Information) pointed toward the formation of a significant amount of phenoxide intermediate prior the QM rearrangement and subsequent elimination,<sup>4a</sup> the kinetics of which could be modeled using eq 2.<sup>10</sup> To a first approximation, the substituent on the methylene group of the QM precursor, i.e., carbonate oxygen atom for **1** versus ether oxygen atom for **2**, was anticipated to have negligible effects on the reactivity of the scissile Si–O bond off the *o*-phenoxy group. Using the  $k_1$  value obtained from **1** as the intrinsic bimolecular rate constant for the Si–O bond cleavage step, the time-dependent fluorescence intensity change from **2** was fitted to derive the 1,4-rearrangement rate constant of  $k_2 = 1.43 \times 10^{-2} \text{ s}^{-1}$ . As anticipated, this unimolecular rate constant was independent of the  $[\text{F}^-]$  ( $= 0.02$ – $0.10 \text{ mM}$ ).<sup>9</sup>

With **1** and **2** serving as convenient rearrangement clocks, we decided to investigate the kinetic consequences of varying the number of QM relays and the pathways sampled from the covalent trigger to the fluorescent reporter. Toward this end, compounds **3** and **4** were prepared and subjected to kinetic studies. Under the same conditions as used for **2** (gray curve, Figure 2b), the *para*-branched **3** involving consecutive 1,4- and 1,6-rearrangements responded much more slowly toward  $\text{F}^-$  (blue curve, Figure 2b) with an effective  $k_2$  value of  $1.38 \times 10^{-3} \text{ s}^{-1}$ . This  $k_2$  parameter in a simplified two-step reaction scheme (eq 2) reflects the collective time delay via two QM rearrangement steps (Scheme 3) and is therefore significantly ( $>10$ -fold) smaller than that ( $1.43 \times 10^{-2} \text{ s}^{-1}$ ) of **2** undergoing only single QM rearrangement. Quite unexpectedly, however, the *ortho*-branched isomer **4** (red curve, Figure 2b) showed a remarkably faster release of the end group compared with **3** (blue curve, Figure 2b). Notably, the exponential growth of the self-fragmentation product from **4** now indicated shifting of the mechanism to  $k_1' \ll k_2$  with the rate-limiting step taken over by the Si–O cleavage reaction ( $k_1 = 159 \text{ M}^{-1} \text{ s}^{-1}$ ) similar to the behavior of **1** (Figures 2a and S3, Supporting Information).

Considering that the *p*- (for **3**) and *o*-QM (for **4**) precursor would have similar propensity toward bond rearrangements, their distinctively different kinetic behavior was difficult to rationalize. More perplexingly, the self-fragmentation of **4** (red curve, Figure 2b) was even *faster* than that of **2** (gray curve, Figure 2b), which is essentially impossible to explain if the chain fragmentation of **4** proceeds via sequential cleavage of the ether followed by the carbonate junction as deduced from the molecular structure (Scheme 3). This counterintuitive observation of a *faster signal relay over a longer distance* suggested the presence of an efficient “shortcut” in self-immolation and immediately called for a complete reconsideration of our initial mechanistic view.

To delineate the molecular basis of this unusually fast signal relay through **4**, an expanded set of compounds **5–8** were prepared and deployed for kinetic analysis. The results summarized in Table 1<sup>11</sup> reconfirmed consistently faster

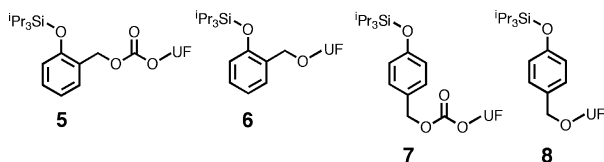
**Table 1.** Kinetic Parameters for Self-Fragmentation of **1–8** (CH<sub>2</sub>Cl<sub>2</sub>, *T* = 293 K)<sup>11</sup>

compound	<i>k</i> <sub>1</sub> (M <sup>−1</sup> s <sup>−1</sup> )	<i>k</i> <sub>2</sub> × 10 <sup>3</sup> (s <sup>−1</sup> )
<b>1</b>	155 <sup>a</sup>	<i>b</i>
<b>2</b>	155 <sup>c</sup>	14.3 <sup>c</sup>
<b>3</b>	155 <sup>c</sup>	1.38 <sup>c</sup>
<b>4</b>	159 <sup>a</sup>	<i>b</i>
<b>5</b>	54 <sup>a</sup>	<i>b</i>
<b>6</b>	54 <sup>d</sup>	6.3 <sup>d</sup>
<b>7</b>	53 <sup>a</sup>	<i>b</i>
<b>8</b>	53 <sup>e</sup>	5.4 <sup>e</sup>

<sup>a</sup> Fitted using eq 1 under pseudo-first-order conditions with *k*<sub>1</sub>' = [F<sup>−</sup>]<sub>0</sub>*k*<sub>1</sub>.

<sup>b</sup> With *k*<sub>2</sub> ≫ *k*<sub>1</sub>, eq 2 converges to eq 1. <sup>c</sup> Fitted using eq 2 with *k*<sub>1</sub> fixed to that of **1**. <sup>d</sup> Fitted using eq 2 with *k*<sub>1</sub> fixed to that of **5**. <sup>e</sup> Fitted using eq 2 with *k*<sub>1</sub> fixed to that of **7**.

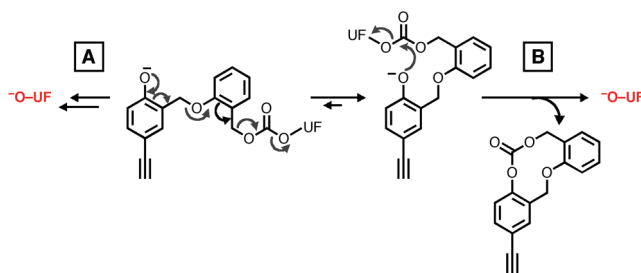
fragmentation rates of the carbonate-linked systems compared with their ether-linked analogues, regardless of the cross-linking pattern, i.e., *ortho* (**5** vs **6**) or *para* (**7** vs **8**). In addition, the rate-limiting Si–O bond cleavage proceeded with comparable *k*<sub>1</sub> values for both *ortho* and *para* isomers (**5** vs **7**) of the carbonate-linked system. Most importantly, the comparable *k*<sub>2</sub> values obtained for **6** and **8** established that *there is no intrinsic difference in the 1,4- vs 1,6-rearrangement rates*, which stands in stark contrast to the behavior of **3** vs **4** shown in Figure 2b.



The simplest and most intuitive explanation for the unusual “ortho effect” in **4** is the operation of an alternative fragmentation mechanism that apparently outperforms the sequential QM rearrangements. As proposed in Scheme 4, the initial Si–O bond cleavage of **4** would generate the phenoxy intermediate. In addition to taking the anticipated repetitive 1,4-rearrangement route (pathway A), this intermediate could adopt a conformation that brings the scissile benzylic carbonate group into a position

(11) For compounds **3**, **6**, and **8**, kinetic data at initial stages of the reaction suffer excessively from interference of multiple intermediates that build up and decay simultaneously.<sup>10</sup> As such, intensity changes at *t* > 40 s were used to derive an effective *k*<sub>2</sub> value from global fitting of five independent data sets to approximate the time delay between the initial Si–O bond cleavage event and the eventual release of the final product umbelliferone.

**Scheme 4.** Chain Fragmentation by Repetitive QM Rearrangement and Elimination (A) or by Direct Nucleophilic Attack (B)



for direct nucleophilic attack by the phenoxide group (pathway B) to release the reporter group. If this alternative signal relay proceeds faster than the conventional QM rearrangements, this unified mechanistic model could fully account for the highly unusual kinetic behavior of the **4**.<sup>12</sup> Fragmentation of the geometrically constrained *para*-linked isomer **3**, on the other hand, can proceed only through stepwise rearrangements (Scheme 3), thereby resulting in slower kinetics than **2** or **4** (Figure 2b). In support of this notion, high-resolution MS analysis of the products obtained from the reaction between **4** and F<sup>−</sup> indeed identified the internal cyclization product from a direct nucleophilic attack (Figure S5, Supporting Information).<sup>9,13</sup>

In summary, a systematic investigation of well-defined small molecules suggested the operation of a dual mechanism in controlled chain fragmentation reactions. For long-lived intermediates with appropriate conformational bias, direct nucleophilic attack can kinetically outperform stepwise bond rearrangements. Alternative design principles capitalizing on such an efficient signal relay cascade can readily be envisioned for stimuli-responsive molecules and materials, which are currently being investigated in our laboratory.

**Acknowledgment.** This work was supported by the U.S. Army Research Office (W911NF-07-1-0533). D.L. is an Alfred P. Sloan Research Fellow.

**Supporting Information Available:** Synthesis and characterization of **1–8** and kinetic measurements and data analysis. This material is available free of charge via the Internet at <http://pubs.acs.org>.

OL900433G

(12) A conceptually related intramolecular nucleophilic attack of “unmasked” phenoxide and subsequent liberation of fluorophore has previously been reported: Chandran, S. S.; Dickson, K. A.; Raines, R. T. *J. Am. Chem. Soc.* **2005**, *127*, 1652–1653.

(13) HR-MS: calcd for [M + H]<sup>+</sup> 281.0808, found 281.0803. Full characterization of the reaction products from preparatory scale reaction was hampered by the high dilution (1.0 μM) required to simulate the reaction conditions in which the kinetic measurements were carried out.